



RESEARCH LETTER

10.1002/2016GL071672

Key Points:

- A new τ_c magnitude relationship using all P wave time windows without saturation for events with $M < 7.5$
- The relationship provides a better magnitude prediction than that derived from 3 s P wave information
- The relationship is expected to improve EEWs performance with fewer false alarms, especially for small earthquakes

Supporting Information:

- Supporting Information S1

Correspondence to:

C. Y. Peng,
pengchaoyong@cea-igp.ac.cn

Citation:


Peng, C. Y., J. S. Yang, Y. Zheng, X. Y. Zhu, Z. Q. Xu, and Y. Chen (2017), New τ_c regression relationship derived from all P wave time windows for rapid magnitude estimation, *Geophys. Res. Lett.*, *44*, doi:10.1002/2016GL071672.

Received 21 OCT 2016

Accepted 9 FEB 2017

Accepted article online 13 FEB 2017

New τ_c regression relationship derived from all P wave time windows for rapid magnitude estimation

C. Y. Peng¹ , J. S. Yang¹, Y. Zheng¹, X. Y. Zhu², Z. Q. Xu¹, and Y. Chen²

¹Real-Time Seismology, Seismological Observation and Interpretation, and Earthquake Forecast, Institute of Geophysics, China Earthquake Administration, Beijing, China, ²Key Laboratory of Earthquake Prediction, Institute of Earthquake Science, China Earthquake Administration, Beijing, China

Abstract Two issues related to the average period τ_c early-warning parameter are the magnitude saturation effect on large earthquakes and considerable scatter for small earthquakes. To reduce the effect of these two issues on earthquake early-warning systems, we introduce a new τ_c regression relationship derived from all P wave time windows (PTWs) in high-pass filtered ($T = 0.075$ Hz) strong-motion data for three damaging moderate-to-large earthquakes. Our results show that this relationship provides a better and more stable magnitude prediction than those derived from 3 s PTW without a saturation effect on large earthquakes with $M < 7.5$. It is expected that fewer false alerts (those outside the magnitude uncertainty tolerance) would be issued. Additionally, a reduction of the initial PTWs to 1–2 s and evolutionary calculation with an expanding window allow more lead time for small-to-moderate events.

1. Introduction

It is not feasible to predict an earthquake in the short term, but we can mitigate seismic damage using earthquake early-warning systems (EEWSs). An EEWS can issue alert messages to the target sites immediately after a destructive earthquake occurs and before the arrival of damaging S waves using rapidly determined source parameters and magnitude based on real-time data recorded by dense seismic arrays. After several decades of development, EEWSs for real-time earthquake hazard mitigation are now operational in many countries worldwide, such as Japan [Nakamura, 1988; Hoshiba et al., 2008], Turkey [Erdik et al., 2003; Sesetyan et al., 2011], Taiwan [Chen et al., 2015; Hsu et al., 2016], Mexico [Espinosa-Aranda et al., 2009], and Romania [Allen et al., 2009]. EEWSs are in the development and testing stages in southern Italy [Satriano et al., 2011], California [Allen et al., 2009; Kuyuk et al., 2014], China [Peng et al., 2011; Peng et al., 2015; Zhang et al., 2016], Iran [Reza et al., 2013], northeastern Italy, Slovenia and Austria [Picozzi et al., 2015a], and southern Iberia [Picozzi et al., 2015b].

An EEWS relies on the seismic network deployment and the distance between the source and the target sites that need to be alerted. There are two main types of EEWSs, i.e., regional and onsite systems. With respect to the former, traditional seismological methods are adopted to rapidly determine source parameters and to estimate the ground motion in other more distant regions. In an onsite EEWS, the initial P wave signal at a single seismic station or an array is analyzed to estimate the ensuing peak ground shaking at the same site. Generally, the regional warning can provide more reliable results and reduce the rate of false alarms because more triggered stations are combined for early-warning parameter calculation. Since it is more time consuming, this approach cannot be used for regions near the epicenter. An onsite EEWS is less reliable, but it can produce rapid warning for sites very close to the epicentral areas, where an early alert is most necessary.

One early-warning parameter, the so-called average period τ_c , calculated from the frequency content of the P phase, was proposed by Wu and Kanamori [2005b] to rapidly estimate the magnitude. This parameter is usually obtained from the vertical component of strong-motion acceleration waveforms or broadband velocity records within a fixed time window after the P wave signal. Based on earthquakes that occurred in different regions around the world, many researchers have discovered that an empirical regression relationship exists between τ_c and the magnitude of an earthquake [e.g., Wu and Kanamori, 2008; Shieh et al., 2008; Wang et al., 2009; Zollo et al., 2010; Peng et al., 2014]. However, only the initial part of the P wave signals of ground motion records, usually within a fixed P wave time window (PTW, 3 or 4 s), was used to derive these empirical relationships. Magnitude saturation is expected when estimating the magnitude of large earthquakes ($M > 7.0$). To overcome this shortcoming, Colombelli et al. [2012] used progressively increasing

PTWs and epicentral distances to finally obtain an estimate of M 8.4 for the 2011 destructive M_w 9 Tohoku-Oki earthquake. This is a significantly better estimate than magnitude estimates based on GPS data and Japan Meteorological Agency (JMA) EEWS using the same time window. Carranza *et al.* [2015] applied this approach to three large earthquakes along the southern Iberian Peninsula and found a similar trend to that reported by Colombelli *et al.* [2012]. However, the regression relationships used in these studies were based on fixed PTWs (3 or 4 s) after the P wave arrival.

In addition, using stations for which T_s (the theoretical S wave arrival) $- T_p$ (the P wave arrival) yielded a lower value than the fixed PTW selected to derive the relationships may result in a systematic error in magnitude estimations owing to a different τ_c versus M scaling for S waves [Lancieri and Zollo, 2008; Lancieri *et al.*, 2011]. Therefore, to further reduce the saturation effect on magnitude estimation and to avoid including the S wave in the regression relationships, a different τ_c empirical relationship needs to be derived.

A Butterworth filter with a high-pass frequency of 0.075 Hz and two poles is usually applied for determination of early-warning parameters. Shieh *et al.* [2008] stated that different pole selections for the Butterworth filter would introduce different uncertainties in magnitude estimation, and processing data using two poles produced the best magnitude estimates for τ_c with 3 s PTW; however, the data set used in their study may be too small (only 16 events with M_w between 6.0 and 8.3). Are their results suitable for deriving regression relationships using more events, especially those with a magnitude smaller than 6.0?

In this paper, we focus on determining a new τ_c empirical regression relationship and the effect of the applied waveform filter on this relationship. To derive a new relationship, our analysis was based on all P wave time windows (APTWs), defined as the window period starting from the trigger time of the P wave until the arrival of the S wave. It is shown that our new τ_c relationship is more robust for magnitude estimation than that obtained from 3 s PTW, and we did not observe saturation when using it to estimate the magnitude of large earthquakes with $M < 7.5$.

2. Data

We used a data set from 2007 to 2014, obtained from the strong-motion networks operated by the China Earthquake Administration. The sampling rates were 200 samples per second and 250 samples per second for some of the mobile stations. The magnitudes of all the used events were reported in catalogs provided by the China Earthquake Networks Center. We usually selected the surface magnitude (M_s) as the reported magnitude for earthquakes with $M \geq 4.0$, and its saturated value was approximately 8.5. According to Kanamori [1977], M_w is related to M_s and agrees very well with M_s for many earthquakes with $M < 8.5$. Owing to a lack of strong-motion records in the magnitude range between 6.5 and 8.0, we added 35 events collected from the K-NET and KiK-net databases ($6.5 \leq M_{JMA} \leq 8.0$) to our data set. From a comparison between M_{JMA} and M_s , Tsuboi [1954] and Bormann *et al.* [2007] found negligible differences between these two scales with a magnitude ranging from 4 to 8. Therefore, in this work, both types of magnitudes are simply denoted as M .

We used four types of event selection criteria: (a) $M \geq 4.0$, (b) hypocenter distances < 200 km, (c) availability of at least three strong-motion station records for each earthquake, and (d) peak ground acceleration (PGA) values of the vertical component record > 0.1 m/s². The last criterion helps to increase the signal-to-noise ratio (SNR) and to reduce the large scatter of τ_c values. In addition, it lowers the number of smaller-magnitude events because our data were dominated by low-magnitude recordings. In total, we used 2773 three-component strong-motion records from 285 events (Table S1 in the supporting information). Figure S1 shows the distribution of the selected strong-motion records with magnitude and the hypocentral distance.

To compute the early-warning parameter τ_c , we used vertical component accelerometer waveforms. The records were detrended, and P and S waves were manually picked. The acceleration signals were then integrated once and twice for obtaining the velocities and displacements, respectively. After the integration process, the displacements were recursively processed using a one-way Butterworth filter with a high-pass frequency of 0.075 Hz and two poles for removing the low-frequency drift. The τ_c was determined in APTWs. For comparison, we also computed τ_c using 3 s PTW after the P wave arrival, similar to other studies [Wu and Kanamori, 2008; Wang *et al.*, 2009; Zollo *et al.*, 2010; Colombelli *et al.*, 2012; Peng *et al.*, 2014].

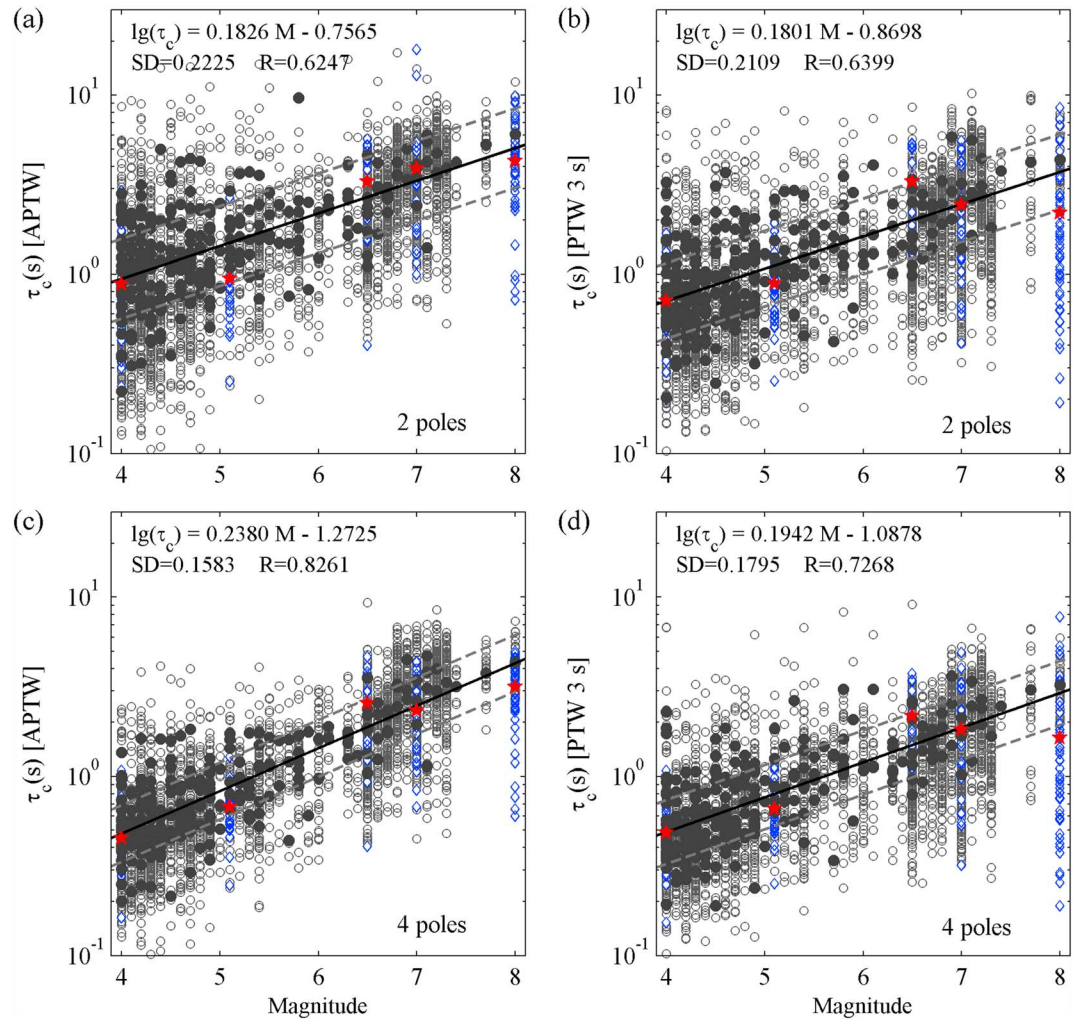


Figure 1. Scaling relationships between the magnitude and τ_c estimated from (a, c) the whole PTW and (b, d) the 3 s PTW. The τ_c values of Figures 1a and 1b were filtered using a 0.075 Hz casual Butterworth high-pass filter with two poles, while those of Figures 1c and 1d were processed using a similar filter with four poles. Open circles represent the τ_c values of strong-motion records, and solid circles indicate the average τ_c measurements from data of the same events. The τ_c values and the average τ_c values obtained from waveform data of the 2008 Wenchuan, the 2013 Lushan, the 2014 Ludian, and two small earthquakes were drawn as blue diamonds and red stars, respectively. The solid line shows the empirical relationships determined in this study, with one standard deviation shown by two dashed lines. SD represents the standard deviation, and R is the correlation coefficient.

3. New Regression Relationship for τ_c Versus Magnitude

To obtain the relationships between the average period τ_c and the magnitude M , the τ_c values for each event were averaged to obtain its arithmetic mean [Wu and Kanamori, 2005a]. We adopted the equation $\log(\tau_c) = AM - B$, where τ_c is determined in seconds and M denotes the magnitude. The results are displayed in Figures 1a and 1b. For both types of relationships, the coefficients, standard error, and correlation were nearly similar to each other. Although the relationship between $\log(\tau_c)$ and M was approximately linear, the scatter was considerable, especially for small earthquakes with $M \leq 5.5$. This trend is the same as that presented in Wu and Kanamori [2005b], Wu et al. [2007], Yamada and Mori [2009], and Zollo et al. [2010]. In order to reduce the scatter, we used a Butterworth filter with four poles. The results are shown in Figures 1c and 1d. Both types of relationships were improved, including the slope, scatter, standard error, and correlation. The results are slightly different from those obtained by Shieh et al. [2008]. When compared with Figures 1a and 1b, we noticed that relationships derived from data filtered using four poles had a larger slope and a lower scatter, while others processed using two poles resulted in a smaller slope and a larger scatter. This may have been

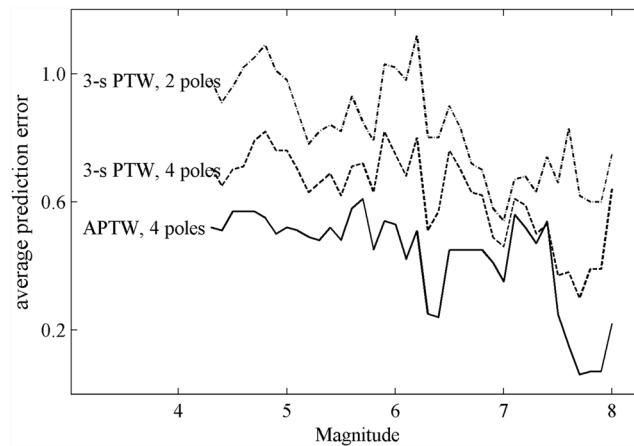


Figure 2. Running averages of magnitude prediction errors as a function of magnitude for newly derived τ_c relationships using APTWs and filtered with four poles (solid line), 3 s PTW and filtered with four poles (dashed line), and 3 s PTW and filtered with two poles (dash-dotted line). The fixed subset size for obtaining the running averages was 0.4 magnitude.

supporting information. Generally, the magnitude estimation obtained using relationships derived from data filtered using four poles was more accurate than that obtained using the relationships based on data filtered using two poles. Moreover, the new τ_c relationship yielded the best estimates compared with other relationships for earthquakes within the selected magnitude range, especially for small events with magnitude less than 5.5. Hence, we infer that the use of the new τ_c relationship is expected to increase the performance of both onsite and regional EEWs by producing more accurate magnitude estimates and by decreasing the rate of false alarms. Here a false alarm is defined as the absolute magnitude estimation error greater than one standard error of the new relationship.

4. Off-Line Application for Earthquakes With Different Mechanisms

To determine the reliability of this new relationship for earthquakes with different mechanisms, we applied it to three damaging earthquakes that occurred in China, i.e., the 2008 Wenchuan M_s 8.0 earthquake, the 2013 Lushan M_s 7.0 earthquake, and the 2014 Ludian M_s 6.6 earthquake (see Table S2 in the supporting information), and to two small events with a magnitude less than 5.5 that were recorded at more than 10 strong-motion stations. The τ_c values and the average τ_c values for each event are shown in Figure 1 as blue diamonds and red stars, respectively. Here to rapidly estimate the magnitudes of these events, τ_c values were reordered with time starting from the occurrence time (OT) of the event, similar to real EEWs. For each triggered station, we estimated the magnitude with progressively expanding PTWs at a regular interval of 1 s after the P wave arrived until it reached APTW. Shorter PTWs were used for stations near the source, and longer PTWs were used for stations at greater distances. The results are presented in Figure 3, shown as black circles, while τ_c measurements of each individual station evolving with expanding PTWs are plotted in Figure S3. The saturation effect on the τ_c values in short PTWs was quite obvious from the results of the three moderate-to-large events, especially for the 2008 Wenchuan earthquake. For comparison, we also plotted the corresponding magnitude estimates (asterisks in Figure 3), which were derived based on the coefficients of τ_c versus M (3 s PTW, four poles) shown in Figure 1d and computed using a fixed PTW (3 s).

With progressively increasing time windows and with the inclusion of more stations, the magnitude estimations for all these earthquakes had similar trends and reached a plateau at specified times after OT. For the Ludian earthquake (Figure 3a) and the Lushan earthquake (Figure 3b), the estimated magnitudes reached a respective plateau of 6.6 and 6.9 approximately 10 s after OT. These estimates are close to the values estimated for these two earthquakes, although the latter had a relatively large variation. With a wider PTW and more observations, the estimation for the Ludian earthquake started to increase until it reached another plateau, i.e., 7.0 at 25 s after OT, clearly overestimating the reference M_s value. However, for the Lushan earthquake, the trend was different from that of the Ludian event. The estimated value first decreased and then

caused by including the records of magnitude 4.0–6.0 and by using a different magnitude scale. The new relationship between τ_c measured in APTWs (four poles) and magnitude M had the largest slope, the smallest standard error, and the best correlation relative to the other types of relationships.

To further assess the performance of our new τ_c regression, we examined the difference between the predicted and observed magnitudes. The running averages of the absolute prediction errors are shown in Figure 2. The absolute prediction errors of each event and individual data points as a function of magnitude are compared in Figure S2 in the

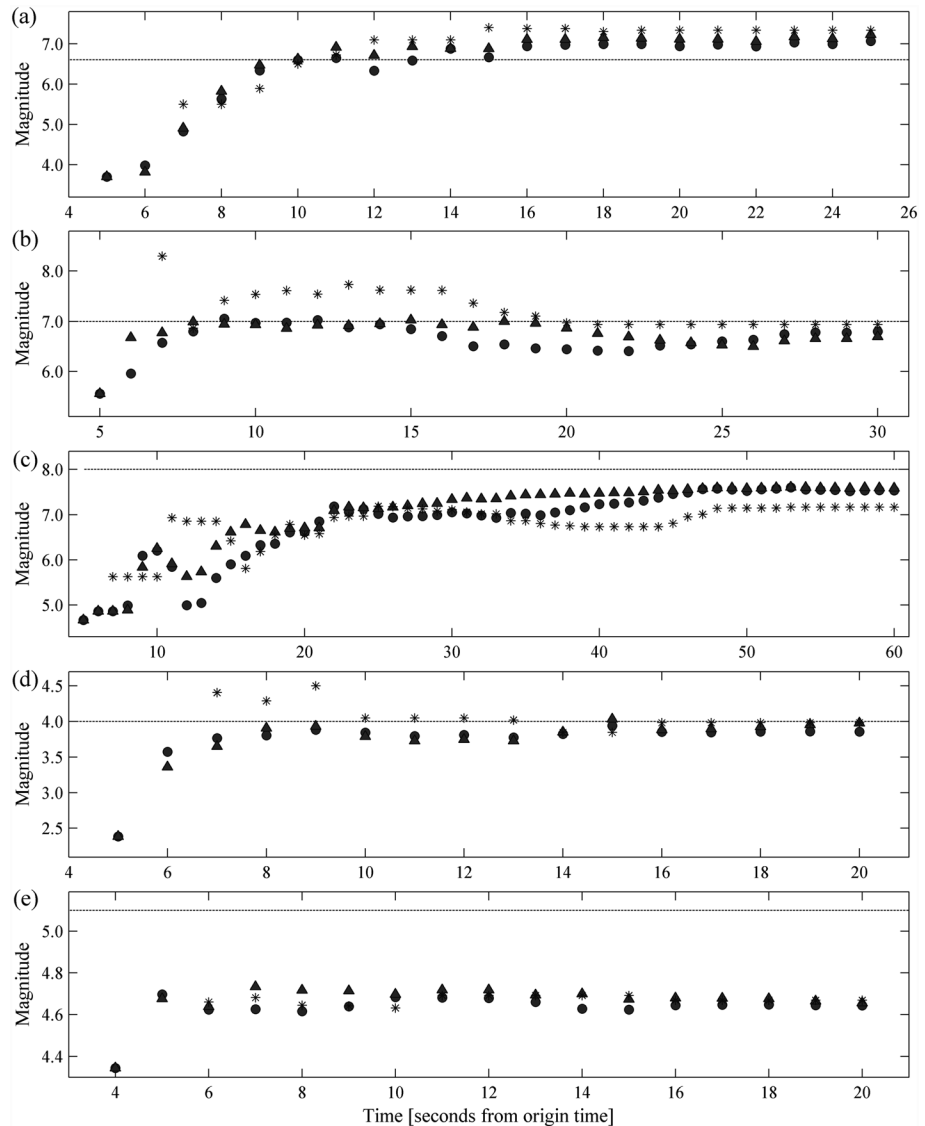


Figure 3. Time evolution of magnitude estimation versus time from the origin time used for the (a) Ludian, (b) Lushan, (c) Wenchuan, and (d, e) two small earthquakes. Circles indicate the estimated magnitudes using standard τ_c average values, and triangles represent the estimated magnitudes calculated by the weighted τ_c average values. Each weight was obtained from the square of the available PTW. Therefore, a longer PTW will contribute more weight to the results of the magnitude estimations. For comparison, in each plot, we also plotted the corresponding magnitude estimates (asterisks), which were derived based on the coefficients of τ_c versus M (3 s PTW, four poles) shown in Figure 1d and computed using a fixed PTW (3 s). The dashed lines show the catalog magnitudes for these earthquakes.

increased until it reached its final plateau (6.8) at 30 s after OT, slightly below the reference value of $M_s = 7.0$. Although the curves of magnitude estimation for these two moderate earthquakes are different from each other, the predicted values between 10 s and the longest time windows after OT are still within one standard error. With respect to the results obtained with τ_c versus M (3 s PTW, four poles), the estimated magnitudes for these two moderate earthquakes had a larger scatter than those derived from the new relationship at the early stage of the rupture when few stations were triggered, especially for the Lushan event (Figure 3b) with a magnitude estimate of 8.3 at 7 s after OT.

The estimated magnitude of the Wenchuan earthquake (Figure 3c) showed a similar behavior to that of the two moderate events but reached its first plateau (7.2) later, approximately 22 s after OT. It then exhibited a small variation from 23 s to 46 s until it reached the final estimated value of 7.6. The final result predicted by

the τ_c versus M (3 s PTW, four poles) relationship was only 7.1, i.e., a significant underestimation of the magnitude of this large earthquake.

For the two small earthquakes, one magnitude estimate obtained from the new relationship (Figure 3d) was significantly more stable than the one derived from the τ_c versus M (3 s PTW, four poles) relationship, and the other (Figure 3e) was comparable to the 3 s PTW result. In addition, we also observed that a PTW of 1–2 s is short enough to obtain a robust estimated magnitude for these two small earthquakes.

To avoid the possible risk of magnitude underestimation resulting from stations with short PTWs, we adopted the method proposed by *Colombelli et al.* [2012]. This method calculates the weighted averages of τ_c values at each considered time step (dark triangles in Figure 3) using the equation as follows:

$$\tau_{c-wa} = \left[\sum_{i=1}^N \log(\tau_{c_i}) \times \text{length}(\text{PTW}_i)^2 \right] / \sum_{i=1}^N \text{length}(\text{PTW}_i)^2$$

where τ_{c-wa} represents the weighted averages of τ_c values at each considered time step, and N is the number of current available triggered stations. Because of the large variability of the τ_c parameter calculated from only a few stations, no evident effect was found on the initial τ_c average values using this method. However, as the PTW was increased and more stations were included, this approach produced more robust and stable results with a smaller variation range, especially for the Wenchuan earthquake. As shown in Figure 3c, no variation was observed between 23 s and 46 s, and we obtained an estimated magnitude of 7.5 at 37 s after OT, which is approximately 10 s faster than that obtained without weighting.

5. Summary and Conclusions

An issue that exists in EEWs is the saturation effect of early-warning parameters on large earthquakes ($M > 7.0$), because the used relationships are always derived from initial P wave information from ground motion records in a predefined time window (usually 3 to 4 s) with magnitude up to 7–7.5 [*Rydelek et al.*, 2007; *Wu et al.*, 2007] and hypocentral distance up to 50–60 km [*Zollo et al.*, 2010; *Colombelli et al.*, 2012, 2014]. Another issue related to the relationships is that the ground motion records in which the arrival times of the theoretical S waves occur within a fixed PTW are also used to derive the relationships. Their inclusion may lead to a significant bias when used to estimate an earthquake magnitude due to different scalings between τ_c and magnitude for P and S waves, for instance, the scalings proposed by *Zollo et al.* [2006]. Therefore, to reduce the saturation effect and avoid S wave contamination in the empirical regression relationships, in this study, a new methodology based on APTWs of strong-motion records was proposed to derive a new τ_c regression relationship for magnitude estimation.

Here for comparison, we used two types of high-pass Butterworth filters to process the τ_c parameter. One filter, which consisted of two poles, is typically used in current EEWs, while the other filter has four poles. The results showed that the relationship between τ_c measured in the APTWs (four poles) and the magnitude M was the best, i.e., with the largest slope, the smallest standard error, and the best correlation compared with the other relationships. This result is slightly different from that obtained by *Shieh et al.* [2008]. The reason may be that the statistical sample size used by *Shieh et al.* [2008] to determine the relationships was too small (only 16 events), and only earthquakes with M_w ranging from 6.0 to 8.3 were used. For this small range of magnitude, no apparent dependence can be found between frequency-based parameters and magnitude, and the correlation is ambiguous, as pointed out by *Rydelek and Horiuchi* [2006] and *Wu and Kanamori* [2008]. Another important result is that the τ_c (APTW, four poles) versus M relationship can yield more robust magnitude estimates for events within the selected magnitude range, especially for small events with $M < 5.5$, and can be compared to T_{\log} [*Ziv*, 2014]. Thus, using this newly derived relationship in existing EEWs, their performance is expected to be enhanced with considerably fewer false alarms.

We used three moderate-to-large damaging earthquakes and two small earthquakes to validate this new τ_c relationship using off-line real-time simulation. Although the test data set is limited, these five events are representative of earthquakes that have occurred in China, especially the three damaging earthquakes. The results show that for the two moderate events, about 8–10 s after OT is required to produce a stable magnitude estimation (3–6 s PTWs), while for the Wenchuan earthquake, a longer time period (approximately 35–40 s after OT, 15–20 s PTWs) is needed because of a relatively long rupture process and more complex

frequency-dependent rupture history. As for the two small earthquakes, which generally had a source radius of approximately 0.8–3 km [Colombelli and Zollo, 2015], it is unnecessary to obtain an estimated magnitude with a 3 s PTW, and only a short PTW (1–2 s) is required to produce a robust magnitude estimate. These results are in full agreement with those obtained by Colombelli *et al.* [2014, 2015]. Additionally, no obvious saturation effect was found for the two moderate earthquakes, and only a small effect with a difference of 0.4 magnitude was observed in the magnitude estimation for the M_s 8.0 Wenchuan giant earthquake. Moreover, when compared with the results obtained from the τ_c versus M (3 s PTW, four poles) relationship, both the earliest and later alerts were more accurate using the new relationship. Furthermore, this relationship reduced the τ_c scatter for the earliest alerts issued, as well as for the final alerts using longer PTWs.

However, it should be noted that τ_c scatter remains an issue for these early P wave EEW methodologies, especially for the earliest alerts, and scatter in short-window τ_c values in real time may have an impact on false alerts that cannot be assessed in this work. Although data for this study were preselected based on the SNR, which can only be achieved in off-line analysis (i.e., using values not available in real time), the influence of this criterion on stable magnitude estimation can be ignored because it will not exclude records close to the epicentral areas, and we will pay more attention to these records in real EEWs. Furthermore, the saturation observed for the 2008 Wenchuan earthquake may be related to the 0.075 Hz cutoff frequency. According to Brune's source spectral model [Brune, 1970], at a stress drop of 3 MPa (i.e., a global average value) and a V_S of 3 km/s, the corner frequencies for magnitudes 7.5 and 8 are 0.0363 Hz and 0.0204 Hz, respectively. Of course, these estimates are the results of simplifications that are likely not adequate to reproduce the real source properties. Nevertheless, this simple example shows us that using a 0.075 Hz cutoff frequency is unlikely to be able to capture the necessary information to correctly estimate the magnitude above a 7.5 magnitude event. In our future work, we will use high-pass Butterworth filters with different cutoff frequencies to analyze their effects on the magnitude estimation for large earthquakes.

With respect to timing performance, although the new relationship was derived from APTWs, it can also be applied to real-time magnitude estimation with progressively expanding PTWs after P wave detection. Using this newly derived relationship, the time used to estimate the magnitude can even be started from the second immediately after the P wave is detected, as compared to the regular procedures using measurements in a fixed PTW (3 or 4 s). From Figure 3, we can infer that a reduction of the initial τ_c window length to 1–2 s and evolutionary calculation with an expanding window allow more lead time to be obtained for small-to-moderate events, while longer PTWs are necessary to produce more robust results for large earthquakes.

When using this new relationship in an EEWs, one possible risk is S wave contamination. In order to avoid S wave inclusion, some automatic S wave detection algorithms can be introduced, such as those proposed by Rosenberger [2010] and Amoroso *et al.* [2012]. However, due to the considerable uncertainties of these automatic S wave detection methods, a simpler approach proposed by Colombelli *et al.* [2014] may be more suitable for avoiding S wave inclusion in the APTW because EEWs applications do not require accurate identification of the S wave arrival time. Using this method, the expected arrival time of the S wave at each station (T_S) can be estimated from the derived relationship $T_S = T_P - bR$ after the hypocentral distance R is roughly determined. Here T_P indicates the onset time of the observed P wave, and b is obtained according to a linear regression after manually checking the arrival times of the S waves from the used data set. To ensure that the probability of including the S wave is very small, the calculated $T_S - T_P$ time can be reduced by 20%.

References

- Allen, R. M., P. Gasparini, O. Kamigaichi, and M. Böse (2009), The status of earthquake early warning around the world: An introductory overview, *Seismol. Res. Lett.*, 80(5), 682–693, doi:10.1785/gssrl.80.5.682.
- Amoroso, O., N. Maercklin, and A. Zollo (2012), S -wave identification by polarization filtering and waveform coherence analyses, *Bull. Seismol. Soc. Am.*, 102(2), 854–861, doi:10.1785/0120110140.
- Bormann, P., R. F. Liu, X. Ren, R. Gutdeutsch, D. Kaiser, and S. Castellaro (2007), Chinese National Network Magnitudes, their relation to NEIC magnitudes, and recommendations for New IASPEI magnitude standards, *Bull. Seismol. Soc. Am.*, 97(1B), 114–127.
- Brune, J. N. (1970), Tectonic stress and the spectra of seismic shear waves from earthquakes, *J. Geophys. Res.*, 75, 4997–5009, doi:10.1029/JB075i026p04997.
- Carranza, M., E. Buforn, and A. Zollo (2015), Testing the earthquake early-warning parameter correlations in the southern Iberian Peninsula, *Pure Appl. Geophys.*, 172(9), 2435–2448, doi:10.1007/s00024-015-1061-6.
- Chen, D.-Y., N.-C. Hsiao, and Y.-M. Wu (2015), The earthworm based earthquake alarm reporting system in Taiwan, *Bull. Seismol. Soc. Am.*, 105(2A), 568–579, doi:10.1785/0120140147.

Acknowledgments

The acceleration seismograms used in this research were provided by the China Strong Motion Networks Center and the Japanese National Research Institute for Earth Science and Disaster Prevention. The Chinese waveform data can be downloaded from <http://222.222.119.9/index.asp> (last accessed in June 2016), while the Japanese waveform data can be obtained from <http://www.kyoshin.bosai.go.jp/> (last accessed in July 2016). The network catalogs for the used events were retrieved from <http://www.csdnmc.ac.cn/newweb/data.htm> (last accessed in June 2016). We would like to express our gratitude to the three anonymous reviewers for their insightful comments and suggestions. This research was cofunded by the National Natural Science Foundation of China (41404048) and the Special Fund of the Institute of Geophysics, China Earthquake Administration (DQJ15C04).

- Colombelli, S., and A. Zollo (2015), Fast determination of earthquake magnitude and fault extent from real-time *P*-wave recordings, *Geophys. J. Int.*, *202*, 1158–1163, doi:10.1093/gji/ggv217.
- Colombelli, S., A. Zollo, G. Festa, and H. Kanamori (2012), Early magnitude and potential damage zone estimates for the great M_w 9 Tohoku-Oki earthquake, *Geophys. Res. Lett.*, *39*, L22306, doi:10.1029/2012GL053923.
- Colombelli, S., A. Zollo, G. Festa, and M. Picozzi (2014), Evidence for a difference in rupture initiation between small and large earthquakes, *Nat. Commun.*, *5*, 3958, doi:10.1038/ncomms4958.
- Colombelli, S., A. Caruso, A. Zollo, G. Festa, and H. Kanamori (2015), A *P* wave-based, on-site method for earthquake early warning, *Geophys. Res. Lett.*, *42*, 1390–1398, doi:10.1002/2014GL063002.
- Erdik, M., Y. Fahjan, O. Ozel, H. Alcik, A. Mert, and M. Gul (2003), Istanbul earthquake rapid response and the early warning system, *Bull. Earthquake Eng.*, *1*, 157–163.
- Espinosa-Aranda, J. M., A. Cuellar, A. Garcia, G. Ibarrola, R. Islas, S. Maldonado, and F. H. Rodriguez (2009), Evolution of the Mexican Seismic Alert System (SASMEX), *Seismol. Res. Lett.*, *80*(5), 694–706, doi:10.1785/gssrl.80.5.694.
- Hoshiba, M., O. Kamigaichi, M. Saito, S. Tsukada, and N. Hamada (2008), Earthquake early warning starts nationwide in Japan, *Eos Trans. AGU*, *89*(8), 73–74, doi:10.1029/2008EO080001.
- Hsu, T.-Y., H.-H. Wang, P.-Y. Lin, C.-M. Lin, C.-H. Kuo, and K.-L. Wen (2016), Performance of the NCREE's on-site warning system during the 5 February 2016 M_w 6.53 Meinong earthquake, *Geophys. Res. Lett.*, *43*, 8954–8959, doi:10.1002/2016GL069372.
- Kanamori, H. (1977), The energy release in great earthquakes, *J. Geophys. Res.*, *82*, 2981–2987, doi:10.1029/JB082i020p02981.
- Kuyuk, H. S., R. M. Allen, H. Brown, M. Hellweg, I. Henson, and D. Neuhauser (2014), Designing a network-based earthquake early warning algorithm for California: Elarms-2, *Bull. Seismol. Soc. Am.*, *104*, 162–173, doi:10.1785/0120130146.
- Lancieri, M., and A. Zollo (2008), A Bayesian approach to the real-time estimation of magnitude from the early *P* and *S* wave displacement peaks, *J. Geophys. Res.*, *113*, B12302, doi:10.1029/2007JB005386.
- Lancieri, M., A. Fuenzalida, S. Ruiz, and R. Madariaga (2011), Magnitude scaling of early-warning parameters for the M_w 7.8 Topocilla, Chile, earthquake and its aftershocks, *Bull. Seismol. Soc. Am.*, *101*(2), 447–463, doi:10.1785/0120100045.
- Nakamura, Y. (1988), On the urgent earthquake detection and alarm system (UrEDAS), in *Proceedings of the Ninth World Conference on Earthquake Engineering*, vol. VII, pp. 673–678, Jpn. Assoc. for Earthquake Disaster Prev., Tokyo.
- Peng, C. Y., J. S. Yang, B. Xue, X. Y. Zhu, and Y. Chen (2014), Exploring the feasibility of earthquake early warning using records of the 2008 Wenchuan earthquake and its aftershocks, *Soil Dyn. Earthquake Eng.*, *57*, 86–93, doi:10.1016/j.soildyn.2013.11.005.
- Peng, C. Y., J. S. Yang, Y. Chen, X. Y. Zhu, Z. Q. Xu, Y. Zhen, and X. D. Jiang (2015), Application of a threshold-based earthquake early warning method to the M_w 6.6 Lushan earthquake, Sichuan, China, *Seismol. Res. Lett.*, *86*(3), 841–847, doi:10.1785/0220140053.
- Peng, H. S., Z. L. Wu, Y. M. Wu, S. M. Yu, D. N. Zhang, and W. H. Huang (2011), Developing a prototype earthquake early warning system in the Beijing capital region, *Seismol. Res. Lett.*, *82*, 394–403.
- Picozzi, M., L. Elia, D. Pesaresi, A. Zollo, M. Mucciarelli, A. Gosar, W. Lenhardt, and M. Živčić (2015a), Trans-national earthquake early warning (EEW) in north-eastern Italy, Slovenia and Austria: First experience with PRESTo at the CE³RN network, *Adv. Geosci.*, *40*, 51–61, doi:10.5194/adgeo-40-51-2015.
- Picozzi, M., S. Colombelli, A. Zollo, M. Carranza, and E. Buforn (2015b), A threshold-based earthquake early-warning system for offshore events in southern Iberia, *Pure Appl. Geophys.*, *172*, 2467–2480, doi:10.1007/s00024-014-1009-2.
- Reza, H., Z. H. Shomali, and M. R. Ghayamghamian (2013), Magnitude-scaling relations using period parameters τ_c and τ_p^{\max} for Tehran region, Iran, *Geophys. J. Int.*, *192*, 275–284.
- Rosenberger, A. (2010), Real-time ground-motion analysis: Distinguishing *P* and *S* arrivals in a noisy environment, *Bull. Seismol. Soc. Am.*, *100*, 1252–1262.
- Rydelek, P., and S. Horiuchi (2006), Is earthquake rupture deterministic? *Nature*, *442*, E5–E6, doi:10.1038/nature04963.
- Rydelek, P., C. Wu, and S. Horiuchi (2007), Comment on "Earthquake magnitude estimation from peak amplitudes of very early seismic signals on strong motion records" by Aldo Zollo, Maria Lancieri, and Stefan Nielsen, *Geophys. Res. Lett.*, *34*, L20302, doi:10.1029/2007GL029387.
- Satriano, C., L. Elia, C. Martino, M. Lancieri, A. Zollo, and G. Iannaccone (2011), PRESTo, the earthquake early warning system for Southern Italy: Concepts, capabilities and future perspectives, *Soil Dyn. Earthquake Eng.*, *31*, 137–153.
- Sesetyan, K., C. Zulfikar, M. Demircioglu, U. Hancilar, Y. Kamer, and M. Erdik (2011), Istanbul earthquake rapid response system: Methods and practices, *Soil Dyn. Earthquake Eng.*, *31*, 170–180.
- Shieh, J.-T., Y.-M. Wu, and R. M. Allen (2008), A comparison of τ_c and τ_p^{\max} for magnitude estimation in earthquake early warning, *Geophys. Res. Lett.*, *35*, L20301, doi:10.1029/2008GL03561.
- Tsубoi, C. (1954), Determination of the Gutenberg-Richter's magnitude of earthquakes occurring in and near Japan, *J. Seismol. Soc. Jpn., Ser. II*, *7*, 185–193.
- Wang, W. S., S. D. Ni, Y. Chen, and H. Kanamori (2009), Magnitude estimation for early warning applications using the initial part of *P* waves: A case study on the 2008 Wenchuan sequence, *Geophys. Res. Lett.*, *36*, L16305, doi:10.1029/2009GL038678.
- Wu, Y.-M., and H. Kanamori (2005a), Experiment on an onsite early warning method for the Taiwan early warning system, *Bull. Seismol. Soc. Am.*, *95*(1), 347–353, doi:10.1785/0120040097.
- Wu, Y.-M., and H. Kanamori (2005b), Rapid assessment of damaging potential of earthquakes in Taiwan from the beginning of *P* waves, *Bull. Seismol. Soc. Am.*, *95*(3), 1181–1185, doi:10.1785/0120040193.
- Wu, Y.-M., and H. Kanamori (2008), Exploring the feasibility of on-site earthquake early warning using close-in records of the 2007 Noto Hanto earthquake, *Earth Planets Space*, *60*, 155–160.
- Wu, Y.-M., H. Kanamori, R. M. Allen, and E. Hausson (2007), Determination of earthquake early warning parameters, τ_c and P_d , for southern California, *Geophys. J. Int.*, *170*, 711–717, doi:10.1111/j.1365-246X.2007.03430.x.
- Yamada, M., and J. Mori (2009), Using τ_c to estimate magnitude for earthquake early warning and effects of near-field terms, *J. Geophys. Res.*, *114*, B05301, doi:10.1029/2008JB006080.
- Zhang, H. C., J. Xing, Y. X. Wei, J. Li, L. C. Kang, S. C. Wang, L. Z. Huang, and P. Q. Yu (2016), An earthquake early warning system in Fujian, China, *Bull. Seismol. Soc. Am.*, *106*, 755–765.
- Ziv, A. (2014), New frequency-based real-time magnitude proxy for earthquake early warning, *Geophys. Res. Lett.*, *41*, 7035–7040, doi:10.1002/2014GL061564.
- Zollo, A., M. Lancieri, and S. Nielsen (2006), Earthquake magnitude estimation from peak amplitudes of very early seismic signals on strong motion, *Geophys. Res. Lett.*, *33*, L23312, doi:10.1029/2006GL027795.
- Zollo, A., O. Amoroso, M. Lancieri, Y.-M. Wu, and H. Kanamori (2010), A threshold-based earthquake early warning using dense accelerometer networks, *Geophys. J. Int.*, *183*, 963–974, doi:10.1111/j.1365-246X.2010.04765.x.